Spin-Label EPR T_1 Values Using Saturation Recovery from 2 to 35 GHz†

James S. Hyde,*,‡ Jun-Jie Yin,§ Witold K. Subczynski,‡ Theodore G. Camenisch,‡ Joseph J. Ratke,‡ and Wojciech Froncisz||

Department of Biophysics, Medical College of Wisconsin, Milwaukee, Wisconsin 53226, Instrumentation and Biophysics Branch, Center for Food Safety and Applied Nutrition, U.S. Food and Drug Administration, College Park, Maryland 20740, and Department of Biophysics, Faculty of Biotechnology, Jagiellonian University, Krakow, Poland

Received: August 6, 2003; In Final Form: October 8, 2003

EPR saturation-recovery (SR) measurements of the electron spin-lattice relaxation time, T_1, of nitroxide-radical spin probes have been made from 2 to 35 GHz. T_1 values of small water-soluble spin probes increase linearly with microwave frequency throughout the full range of available frequencies. T_1 values of four commonly used hydrophobic probes in lipid bilayers also increase with frequency, but the dependence is weaker and complex. Contributions of dissolved molecular oxygen to relaxation rates were independent of microwave frequency. T_1 values of ^{15}N-containing labels are always somewhat longer than for ^{14}N labels. Details of the Q-band SR spectrometer, which is based on frequency translation technology, are provided. A new way to suppress free induction decay signals in SR experiments has been found: pump and observing frequencies time-locked and separated by about 1 kHz in frequency. A novel three-loop−two-gap resonator with a sample volume of 30 nl was used for the Q-band measurements. It is concluded that Q-band is a favorable frequency for SR spin-label oximetry studies.

1. Introduction

Measurement of EPR spin-lattice relaxation times (T_1) using saturation-recovery (SR) methods has been reviewed by Hyde[1,2] and Eaton and Eaton.[3] There is a general understanding that measurements of T_1 values as a function of microwave frequency should give useful information, not only with respect to mechanisms of relaxation, but also for liquid-phase studies, about molecular dynamics. Experimental data, however, are scant because of the instrumental demands of constructing pulse spectrometers over a range of microwave frequencies.

At the National Biomedical EPR Center, four SR instruments have been constructed at various microwave frequencies. The construction began in 1975, and Q-band capability was added in 2002. One of these instruments was based on an S-band octave-bandwidth microwave bridge operating in the range of 2−4 GHz. Loop-gap resonators were constructed at 2.54 and 3.45 GHz, permitting SR data to be obtained at these two frequencies. SR capability exists also at X-, K-, and Q-bands, resulting in an overall frequency range of about a factor of 15, which is covered by five discrete frequencies.

Measurements of T_1 values for several nitroxide-radical spin probes and spin-label samples using the four lower frequencies were made by J.-J. Yin about a decade ago. These data were reported in abstract form at various meetings, but no formal paper was written. The purpose of the present paper is to place these data into the scientific literature, supplemented by new measurements at Q-band. The latter instrument is based on frequency translation technology and is a departure from the designs of other SR instruments. An additional purpose of the paper is to describe this equipment.

T_1 values are reported for four spin probes that are widely used for research on model membranes as well as biological membranes. Data are also presented on two small water-soluble spin probes. Information on the differences in T_1 values comparing ^{14}N- and ^{15}N-containing spin probes is also presented. In addition, the temperature was varied. Experiments are presented that test the effects of dissolved oxygen on spin-label T_1 values across the frequency range of the SR instruments available to us. The spirit of the paper is to present multifrequency T_1 data empirically with minimal interpretation, very much like the paper by Percival and Hyde,[4] which provides T_1 values for several spin labels at X-band.

2. Methods

Saturation-Recovery Spectrometers. Saturation-recovery data were obtained using four different SR spectrometers, operating at various frequencies from 2 to 35 GHz. The S-band (2−4 GHz), the X-band (8.5−9.6 GHz), and the K-band (18.5−19.5 GHz) microwave circuits are closely related to the one described in refs 5 and 6. The X-band instrument is a dedicated SR spectrometer, whereas SR capability at S- and K-bands was achieved by constructing SR accessories that could be used with continuous wave (CW) reference-arm bridges of conventional configuration.[7,8] The SR microwave circuit used at Q-band differed substantially from the ones used at the other microwave frequencies and is described here in greater detail.

Early SR spectrometers were reviewed by Huisjen and Hyde,[5] who classified them into two categories: those with pump and observing power derived from the same source and therefore coherent, and those derived from two different sources and therefore incoherent. These authors developed a saturation-recovery spectrometer of the coherent type and encountered

† Part of the special issue "Jack H. Freed Festschrift".

* Corresponding author. Phone: (414) 456-4005; fax: (414) 456-6512; e-mail: jshyde@mcw.edu.

‡ Medical College of Wisconsin.

§ U.S. Food and Drug Administration.

|| Jagiellonian University.

10.1021/jp036329z CCC: $27.50
Published on Web 03/30/2004

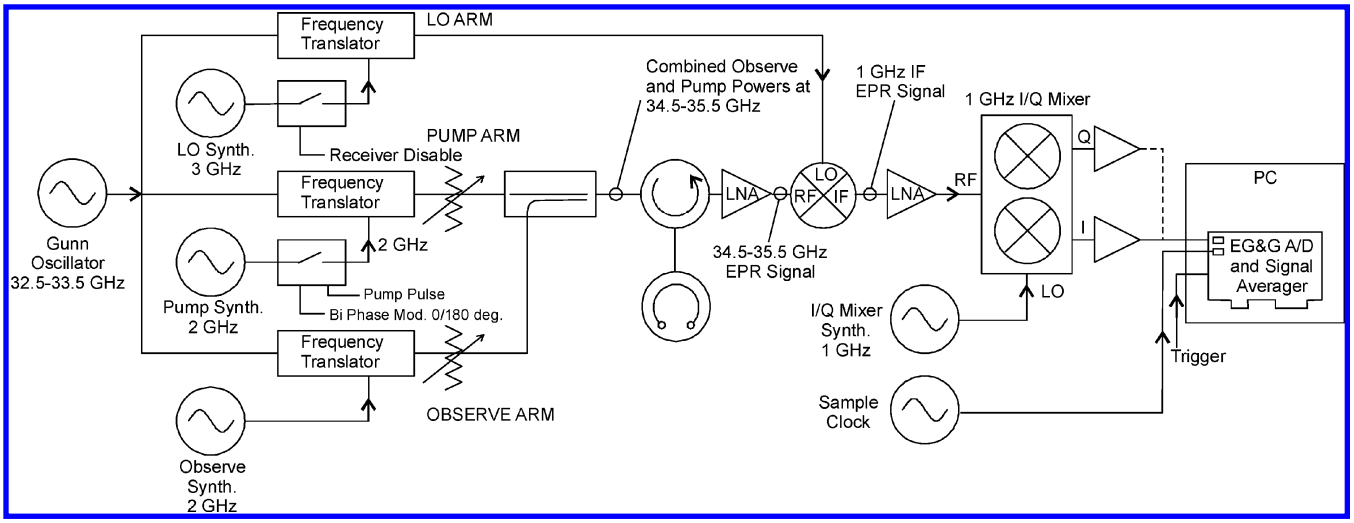

Figure 1. Q-band saturation-recovery microwave circuit.

signals that were a superposition of free induction decay (FID) and SR responses. To separate these signals, they introduced the technique of 180° pump-phase modulation, which modulated the sign of the FID response but not that of the SR response, thereby permitting separation of the superimposed signals. This technique was used in most of the experiments reported here. At S-band, FID signals were extremely intense and an additional method of suppression was employed: artificially broadening the lines using an applied gradient of the static magnetic field over the sample to reduce T_2* and greatly shorten the FID response.

The Q-band SR spectrometer has the capability of 180° pump-phase modulation. However, it also incorporates a new method for FID suppression. The microwave circuit is shown in Figure 1. Pulses are formed at 2 GHz and frequency translated to 34.5−35.5 GHz by mixing with the output of a fundamental low-phase-noise Gunn diode oscillator at 32.5−33.5 GHz. This oscillator was designed in this laboratory by R. A. Strangeway.[9] The observe microwave power is similarly derived from another synthesizer at 2 GHz that is also mixed with a portion of the output of the Gunn diode oscillator. The detection system is superheterodyne. A frequency-offset local oscillator (LO) signal is derived from a 3 GHz synthesizer mixed with a third portion of the Gunn diode output. Detection consists of mixing the Q-band SR signal with the LO to obtain a 1 GHz intermediate frequency (IF). Amplification followed by mixing with a 1 GHz synthesizer-derived signal in an I/Q mixer results in detection of the envelope of the microwave carrier, namely, the SR signal itself.

This bridge design permits FID suppression in a way that is made possible through the use of multiple frequency synthesizers and microwave frequency translations. The pump is locked to the observing source through a common 10 MHz clock, but they can be offset by any desired frequency, typically 1 kHz. Thus, the pump and observing frequencies are neither coherent nor incoherent and free running. Instead, they are locked to each other at a fixed offset. A benefit of this method is that the two frequencies are well within the spin packet width but cannot drift with respect to each other. With the pump and observed frequencies separated by this amount, FID signals are effectively averaged away, leaving only the SR signal. A 180° pump-phase modulator is illustrated in Figure 1, but it no longer needs to be used.

The Q-band bridge as well as the present X-band system use LabView software for field control and data acquisition. The actual pulse data are acquired and averaged by an EG&G Model 9826 card, which is an ISA bus card in a PC. LabView software provides additional averaging. Differencing that is synchronized with field modulation improves the baseline. Biphase modulation is also controlled through this software to suppress the FID signal generated by the pump pulse.

Resonators. Loop-gap resonators (LGR)[10] were used in all experiments of this paper. They are highly advantageous for SR experiments for the following reasons:

- The Q-value is relatively low, substantially decreasing the resonator ringing time.
- Because of the low Q, the intensity of the irradiating field can be relatively high, permitting irradiation of a substantial portion of the spectrum.
- The resonator efficiency parameter Λ (the field produced by one watt of incident power)[11] is high. Thus for a desired irradiation level, the incident RF power is low, which tends to reduce instrumental artifacts that arise when high power is used.
- The small physical size is strongly advantageous for SR experiments in the S-band range where cavity resonators are unreasonably large.
- The filling factor is very high, resulting in good sensitivity even though the Q-value is low.
- The RF field tends to be uniform over the sample, resulting in uniform response throughout the sample.
- The S-band resonator used here is illustrated in Figure 3 of ref 11. The X-band resonator closely follows the design shown in ref 10. Wood et al.[12] introduced the three-loop−two-gap resonator, variations of which were used at both K- and Q-band. The K-band design is shown in ref 13.

At Q-band, LGRs become very small. The first Q-band LGR was described in ref 14. It was an asymmetric two-loop−one-gap configuration with a two-stage microwave transformer: from waveguide to the larger loop and from the larger loop to the smaller sample-containing loop. A new Q-band LGR has recently been developed and is described in more detail here. It is a three-loop−two-gap design shown in Figure 2 and made from aluminum. Gaps were cut using electrical discharge machining (EDM) techniques. The sample volume is about 30 nl. Coupling is similar to that described in ref 10.

Sample Preparation. Dimyristoylphosphatidylcholine (DMPC) was obtained from Sigma (St. Louis, MO), 5-, 12-, and 16-doxylstearic acid spin labels (5-, 12-, 16-SASL) and cholestane spin label (CSL) were from Molecular Probes (Junction City, OR), 3-carbamoyl-2,2,5,5-tetramethyl-3-pyrrolin-1-yloxy (CTPO)

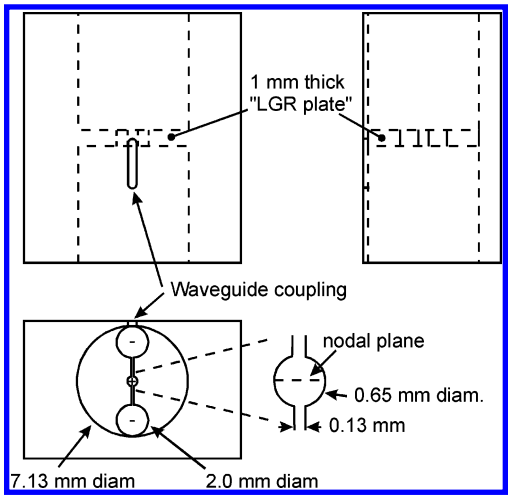

Figure 2. Three-loop−two-gap resonator for Q-band experiments on spin labels.

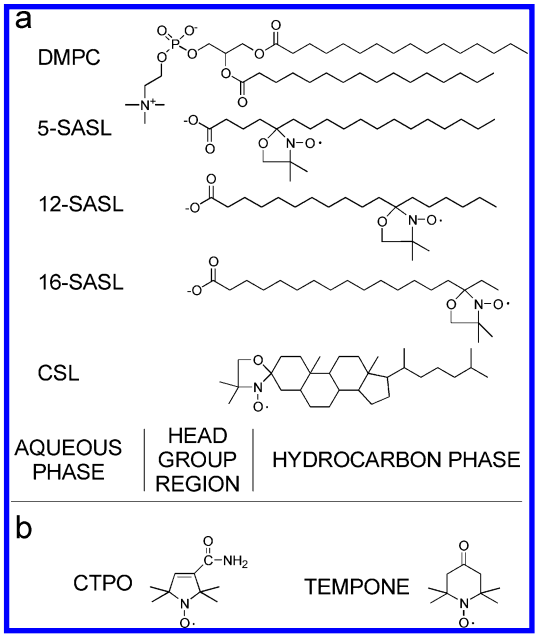

Figure 3. Spin labels used in this work.

and 2,2,6,6-tetramethyl-4-piperidone-1-oxyl (TEMPONE) came from Aldrich Chemical Co. (Milwaukee, WI). The ^{15}N CSL spin label was a gift from Prof. J. H. Park (Vanderbilt University). ^{15}N stearic acid compounds were synthesized by Prof. J. Joseph following the procedures of ref 15. Chemical structures of the lipid spin labels and approximate locations within the DMPC bilayer are shown in Figure 3a. Chemical structures of the water-soluble spin labels are shown in Figure 3b.

The membranes used in this work were multilamellar dispersions of lipids (liposomes) containing 0.5 or 1 mol % of spin labels and were prepared as described earlier.[16] The buffer used was 0.1 M sodium borate at pH 9.5. To ensure that all carboxyl groups of SASL were ionized in DMPC membranes, a rather high pH was chosen. In some experiments, the lipid dispersion was centrifuged briefly and the loose pellet (~20% lipid W/W) was used for EPR measurements. In other experiments, dense liposome dispersions with a final spin-label concentration of 1−3 mM were used. Water solutions of CTPO and TEMPONE were 0.5 mM. Samples were transferred to TPX capillaries or Teflon tubes positioned in the resonator and promptly deoxygenated. For oximetry measurements, the samples

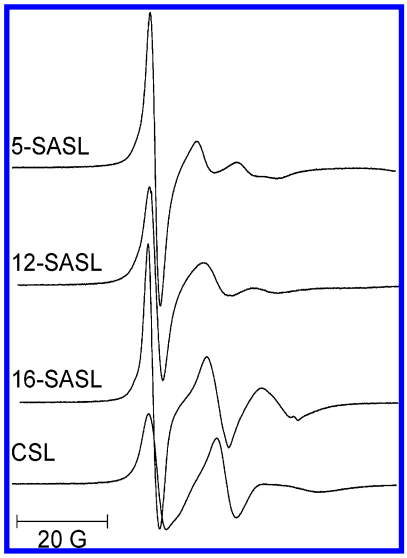

Figure 4. EPR spectra of lipid-soluble spin labels in DMPC bilayers at Q-band (27 °C).

were equilibrated with a mixture of nitrogen and air adjusted with a flowmeter (Matheson Gas Products, model 7631 H-604).[17] The same gas was used for temperature control.

Saturation Recovery Methods. Percival and Hyde[6] emphasized the importance in SR experiments of satisfying the condition

$$\gamma_e^2 B_1^2 T_1 T_2 \ll 1 \qquad (1)$$

where γ_e is the gyromagnetic ratio and $2B_1$ is the amplitude of the microwave magnetic field at the observe frequency. Otherwise, the T_1 will be decreased from its true value. Data reported here satisfy this condition. This problem tends to be less serious in fluid-phase experiments at Q-band than at lower frequencies, because T_2 values tend to be shorter.

For water solutions of CTPO and TEMPONE, the duration of the pulse was 0.3 μs. For membrane suspensions, the pulse duration was 0.3−1 μs.

All recovery times acquired here were single-exponential in character. For CTPO and TEMPONE, concentrations were sufficiently high that the three hyperfine lines were strongly coupled. For the membrane spin probes, motion was sufficiently slow that the nitrogen nuclear relaxation times were shorter than the electron T_1 values, again resulting in strong coupling of the three hyperfine lines.

For Q-band SR, the low-frequency hyperfine line, which is most intense, was observed (Figure 4). At other frequencies, the central line was observed. Frequent control experiments to verify that measured T_1 values were independent of the observed hyperfine line were carried out.

Data Acquisition and Processing. Sampling intervals (4, 8, 16, 32, 20, 40, 60, and 80 ns) depended on sample, temperature, oxygen tension, and microwave frequency. Typically, 8×10^5 decays were averaged, half of which were off-line and differenced for baseline correction, with 256 (for the two S-bands), 512 (for X- and K-bands), and 2048 (for Q-band) data points per decay. Total accumulation time was about 2−5 min. The recovery curves were fitted by single, double, and triple exponentials and compared. The result indicated that for all of the recovery curves obtained in this work, no substantial improvement in the fitting was observed when the number of exponentials was increased from one, establishing that the

TABLE 1: Electron Spin-Lattice Relaxation Times for ^{14}N Spin-Label CTPO and TEMPONE in Water (μs) at 20 °C

frequency (GHz)	^{14}N CTPO	^{14}N TEMPONE
S_1 (2.54)	0.33	0.25
S_2 (3.45)	0.42	0.32
X (9.15)	0.68	0.49
K (18.5)	0.94	0.77
Q (34.6)	1.58	0.92

recovery curves can be analyzed as single exponentials. Fits were based on a damped linear least-squares method.

3. Results

Table 1 shows T_1 values for two small water-soluble spin labels, CTPO and TEMPONE, as a function of microwave frequency. These values are plotted in Figure 5a. The values are substantially shorter than for the lipid-soluble spin labels that have been studied in this work. The values increase approximately as $(\text{frequency})^{1/2}$ throughout the range of available frequencies. CTPO consistently exhibits values that are longer than for TEMPONE by about 30%. We have also observed that rotational correlation times for CTPO are consistently longer than for TEMPONE, over a range of solvents and temperatures.

Table 2 shows all other SR data reported in this paper. Data are shown for four lipid-soluble spin labels in DMPC as a function of microwave frequency. Some T_1 values have been collected for ^{15}N-containing spin labels, which are also shown in the table. Figure 5b, 5c shows plots of these values as a function of microwave frequency in semilog displays. Up to K-band, 18.5 GHz, the plots are well fit to straight lines in these displays, which to the best of our knowledge is a new result and not predicted by existing theory. However, for Q-band, the 12- and 16-SASL deviate from this behavior. (The 5-SASL data appear in both Figure 5b and Figure 5c, but with slightly different curves through the points.) Increase of T_1 values that is observed for spin labels with longer rotational correlation times or at higher microwave frequencies will result in increase of the sensitivity to bimolecular collisions with paramagnetic relaxation agents. The temperature dependence of relaxation times seen in Table 2 establishes criteria for the requisite stability of temperature control in spin-label oximetry studies.

Table 3 illustrates the effect of the nitrogen isotope on relaxation times. Using the data in Table 2, the entries in Table 3 have been calculated using the expression:

$$\%\ \text{decrease} = 2\left\{\frac{[T_1(^{14}N)]^{-1} - [T_1(^{15}N)]^{-1}}{[T_1(^{14}N)]^{-1} + [T_1(^{15}N)]^{-1}}\right\} \times 100 \quad (2)$$

Several points can be made concerning the effect of the choice of isotope on the relaxation times or rates.

- The largest percent changes are found with cholestane. In this label, the pi orbital is perpendicular to the bilayer normal.
- All values are positive, indicating that ^{15}N-containing labels always have longer T_1's than their ^{14}N counterparts.
- Percent changes in relaxation rates tend to decrease as the frequency increases. This effect is particularly evident with the 12-SASL and 16-SASL labels.
- Percent changes with the 5-SASL labels are, in general, much smaller than with the other labels.
- The pattern of entries in Table 3 suggests that measurement of percent changes as a function of microwave frequency can yield insight into molecular motion.

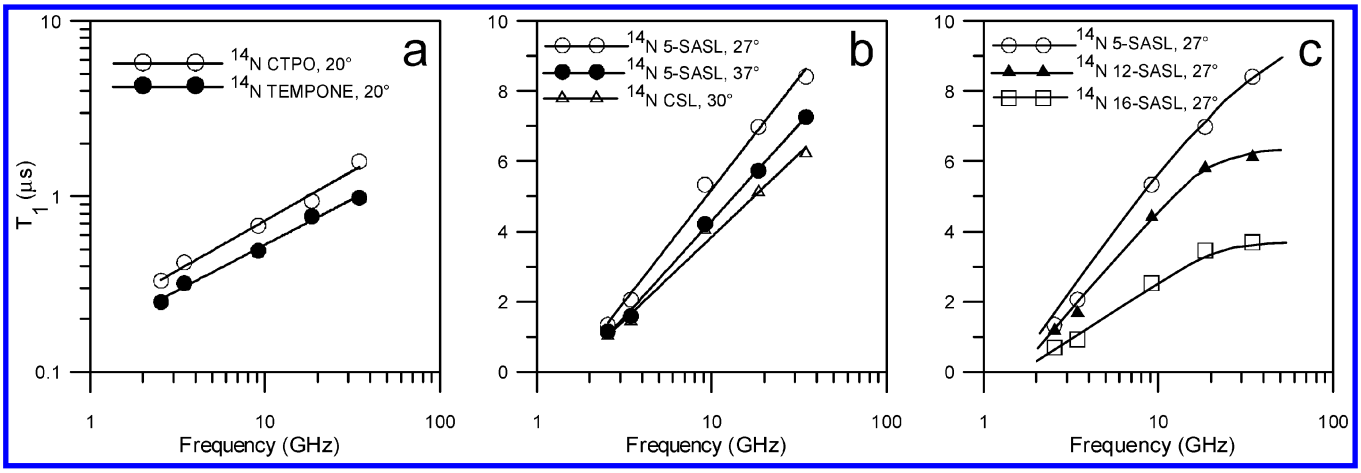

Figure 5. T_1 values vs microwave frequency.

TABLE 2: Electron Spin-Lattice Relaxation Times (μs) for ^{14}N and ^{15}N Lipid Spin Labels in DMPC Bilayers

		^{14}N				^{15}N			
temp. (°C)	freq. (GHz)	5-SASL	12-SASL	16-SASL	CSL[a]	5-SASL	12-SASL	16-SASL	CSL[a]
27	S_1 (2.54)	1.34	1.18	0.69	1.02	1.46	1.35	0.90	1.42
	S_2 (3.45)	2.06	1.67	0.92	1.44	2.18	1.80	1.17	2.02
	X (9.2)	5.33	4.41	2.52	4.05	5.83	4.81	2.80	4.91
	K (18.5)	6.98	5.81	3.46	5.13	7.38	5.99	3.62	6.41
	Q (34.6)	8.41	6.11	3.69	6.22				
37	S_1 (2.54)	1.15	0.99	0.60		1.38	1.11	0.73	
	S_2 (3.45)	1.59	1.35	0.83		2.10	1.48	1.06	
	X (9.2)	4.21	3.62	2.19		4.65	3.91	2.29	
	K (18.5)	5.73	5.08	3.10		6.41	5.28	3.51	
	Q (34.6)	7.26	5.61	3.25					

[a] The data on ^{14}N and ^{15}N CSL were obtained at 30 °C.

TABLE 3: Percent Decrease in Relaxation Rates, Comparing ^{15}N with ^{14}N Spin Labels

frequency (GHz)	$^{14}N-^{15}N$ 5-SASL	$^{14}N-^{15}N$ 12-SASL	$^{14}N-^{15}N$ 16-SASL	$^{14}N-^{15}N$ CSL
S_1 (2.54)	8.5	13.4	26.4	32.8
S_2 (3.45)	5.6	7.6	23.9	33.4
X (9.2)	8.9	8.7	10.6	20.0
K (18.5)	5.8	2.9	4.6	22.2

TABLE 4: Oxygen Transport Parameter versus Microwave Frequency

freq. (GHz)	S_1 (2.54)	S_2 (3.45)	X (9.2)	K (18.5)	Q (34.6)
$T_1(\mu s)$	0.69	0.94	2.54	3.46	3.69
$W(x)$ $(\mu s)^{-1}$	2.68	2.71	2.67	2.54	2.68

Bimolecular collision rates with oxygen have been studied as a function of microwave frequency using ^{14}N 16-SASL in DMPC bilayers at pH 9.5, 27°. Measurements were made as a function of the percent of air in the temperature regulation gas that flowed over the thin-walled plastic sample tube (either TPX or Teflon). Data were expressed as an oxygen transport parameter defined by Kusumi et al.:[17]

$$W(x) = T_1^{-1}(\text{air},x) - T_1^{-1}(N_2,x) \quad (3)$$

where the T_1's are the spin-lattice relaxation times of the nitroxide equilibrated with atmospheric air and nitrogen, respectively. $W(x)$ is proportional to the product of the local translational diffusion coefficient and the local concentration of oxygen (thus $W(x)$ is called a "transport" parameter) at a "depth" x in a lipid bilayer that is equilibrated in the atmospheric air.

Results of this experiment are shown in Table 4. It was established that the effect of bimolecular collisions of oxygen on observed spin-label relaxation rates is independent of microwave frequency. This is a valuable result, since spin-label oximetry is a widely used technique in the contexts of site-directed spin labeling (SDSL)[18,19,20,21] and discrimination by oxygen transport (DOT).[22,23,24]

4. Discussion

A principal application of saturation recovery is spin-label oximetry. There are two broad classes of oximetric studies. Measurements of oxygen accessibility (and also paramagnetic ion accessibility) in a context of SDSL yield protein structural information. The second class is DOT. Membrane domains, often short-lived, can be revealed on the basis of differing solubilities of oxygen in the domains.[22,23,24]

The results of this paper indicate that SR oximetric studies at Q-band can be expected to be advantageous relative to the use of lower microwave frequencies. Because the T_1 values of spin labels are intrinsically longer at Q-band, the sensitivity to bimolecular collisions with oxygen is increased. Additional increase in the intrinsic T_1 value can be obtained by using ^{15}N (Table 3). Often, CW saturation methods are used for spin-label oximetry. Because these studies measure the product T_1T_2, they can be less advantageous at Q-band than at lower frequencies because T_2 tends to be shorter. However, as indicated by eq 1 above, shorter T_2 values are advantageous in SR studies because of the reduced effect of the observing power level on the apparent T_1 value. Moreover, even if there is some effect of the observing power on the apparent T_1 value, the oximetric measurements are not affected.[25] Thus at Q-band, the level of the observing microwave field can be higher than one might expect on the basis of X-band studies, resulting in both a good signal-to-noise ratio and good sensitivity to oxygen.

The data of Table 4 showing that the contribution of bimolecular collisions with oxygen ($W(x)$ values) to T_1^{-1} is independent of microwave frequency and is viewed as particularly significant. There might be concerns that both the Heisenberg exchange rate and the possible direct effect on T_1 during a collision are microwave-frequency dependent, but these effects, if present, are small.

A further benefit of Q-band relative to lower microwave frequencies is that the resonator efficiency parameter, Λ,[11] increases as the 3/4 power of the frequency ratio for a series of scaled but otherwise identical cavity resonators.[26] Microwave power requirements for SR measurements on spin labels at Q-band are modest. Additional increase in Λ to a value that is estimated to be 15 on the basis of ref 14 has been achieved in the present work using the three-loop−two-gap resonator illustrated in Figure 2. This sample volume is about as small as is practical, and thus this value of Λ is believed to be about as high as can be achieved at Q-band. The design is optimum for very small samples. The geometry can be altered by increasing the size of the central sample loop and decreasing the size of the outer loop if larger amounts of sample are available.

The new technique for canceling the FID contamination that is introduced here, namely, locking the observing and pumping frequencies at a fixed offset from each other, appears advantageous. In addition to suppression of the FID, it should be possible simultaneously to suppress the SR signal and detect the FID signal by suitable signal processing prior to averaging of pulse responses. The authors are of the opinion that most SR instruments in future years will be based on extensive use of frequency translation, as illustrated in the microwave circuit of Figure 1.

It is clear that multifrequency measurements of T_1 values constitute an important test of models for T_1 spin-lattice relaxation. Whether such measurements will be found useful in understanding complex anisotropic motions is less clear, although the results in Figure 5c suggest that insight into motions that occur for C12 (12-SASL) and C16 (16-SASL) such as extensive fluctuations toward the membrane surface[27,28,29] can be probed using SR methods. Measurements of $^{14}N-^{15}N$ differences according to eq 2 and Table 3 yield additional motional information.

Acknowledgment. We thank Prof. J. H. Park for the gift of the ^{15}N labeled cholestane and gratefully acknowledge contributions of our colleagues to this work: J. Joseph (^{15}N synthesis of stearic-acid spin labels), R.A. Strangeway (design of the 32.5-33.5 GHz oscillator), and R.R. Mett together with J.R. Anderson (assistance with development of the Q-band loop gap resonator). This work was supported by grants EB002052 and EB001980 from the National Institutes of Health.

References and Notes

(1) Hyde, J. S. In *Time Domain Electron Spin Resonance*; Kevan, L., Schwartz, R. N., Eds.; John Wiley and Sons: New York, 1979; pp 1−30.

(2) Hyde, J. S. In *Foundations of Modern EPR*; Eaton, S. S., Eaton, G. R., Salikhov, K. M., Eds.; World Scientific Publishing: New York, 1998; pp 607−618.

(3) Eaton, G. R.; Eaton, S. S. In *Biological Magnetic Resonance, Vol. 24*; Eaton, S. S., Eaton, G. R., Berliner, L. J., Eds.; Kluwer: Boston, 2004; pp 3−18.

(4) Percival, P. W.; Hyde, J. S. *J. Magn. Reson*. **1976**, *23*, 249−257.
(5) Huisjen, M.; Hyde, J. S. *Rev. Sci. Instrum*. **1974**, *45*, 669−675.
(6) Percival, P. W.; Hyde, J. S. *Rev. Sci. Instrum*. **1975**, *46*, 1522−1529.
(7) Froncisz, W.; Scholes, C. P.; Hyde, J. S.; Wei, Y.-H.; King, T. E.; Shaw, R. W.; Beinert, H. *J. Biol. Chem*. **1979**, *254*, 7482−7484.
(8) Lesniewski, P.; Hyde, J. S. *Rev. Sci. Instrum.* **1990**, *61*, 2248−2250.
(9) Strangeway, R. A.; Ishii, T. K.; Hyde, J. S. *IEEE Trans. Microwave Theory Technol.* **1988**, *36*, 792−794.
(10) Froncisz, W.; Hyde, J. S. *J. Magn. Reson.* **1982**, *47*, 515−521.
(11) Hyde, J. S.; Froncisz, W. In *Advanced EPR: Applications in Biology and Biochemistry*; Hoff, A. J., Ed.; Elsevier: Amsterdam, 1989; pp 277−306.
(12) Wood, R. L.; Froncisz, W.; Hyde, J. S. *J. Magn. Reson.* **1984**, *58*, 243−253.
(13) Oles, T.; Hyde, J. S.; Froncisz, W. *Rev. Sci. Instrum*. **1989**, *60*, 389−391.
(14) Froncisz, W.; Oles, T.; Hyde, J. S. *Rev. Sci. Instrum*. **1986**, *57*, 1095−1099.
(15) Joseph, J.; Lai, C.-S. *J. Labelled Compd. Radiopharm.* **1987**, *24*, 1159−1164.
(16) Kusumi, A.; Subczynski, W. K.; Pasenkiewicz-Gierula, M.; Hyde, J. S.; Merkle, H. *Biochim. Biophys. Acta* **1986**, *854*, 307−317.
(17) Kusumi, A.; Subczynski, W. K.; Hyde, J. S. *Proc. Natl. Acad. Sci. U.S.A.* **1982**, *79*, 964−968.
(18) Feix, J. B.; Klug, C. S. In *Biological Magnetic Resonance, Vol. 14. Spin Labeling: The Next Millennium*; Berliner, L. J., Ed.; Plenum Press: New York, 1998; pp 251−281.
(19) Altenbach, C.; Greenhalgh, D. A.; Khorana, H. G.; Hubbell, W. L. *Proc. Natl. Acad. Sci. U.S.A.* **1994**, *91*, 1667−1671.
(20) Farahbakhsh, Z. T.; Altenbach, C.; Hubbell, W. L. *Photochem. Photobiol.* **1992**, *56*, 1019−1033.
(21) Hubbell, W. L.; Cafiso, D. S.; Altenbach, C. *Nat. Struct. Biol.* **2000**, *7*, 735−739.
(22) Ashikawa, I.; Yin, J.-J.; Subczynski, W. K.; Kouyama, T.; Hyde, J. S.; Kusumi, A. *Biochemistry* **1994**, *33*, 4947−4952.
(23) Kawasaki, K.; Yin, J.-J.; Subczynski, W. K.; Hyde, J. S.; Kusumi, A. *Biophys. J.* **2001**, *80*, 738−748.
(24) Subczynski, W. K.; Kusumi, A. *Biochim. Biophys. Acta* **2003**, *1610*, 231−243.
(25) Hyde, J. S.; Yin, J.-J.; Feix, J. B.; Hubbell, W. L. *Pure Appl. Chem.* **1990**, *62*, 255−260.
(26) Rinard G. A.; Eaton, S. S.; Eaton, G. R.; Poole, C. P., Jr.; Farach, H. A. In *Handbook of Electron Spin Resonance, Vol. 2*; Poole, C. P., Jr.; Farach, H. A., Eds.; AIP Press: New York, 1999; pp 1−23.
(27) Yin, J.-J.; Feix, J. B.; Hyde, J. S. *Biophys. J.* **1987**, *52*, 1031−1038.
(28) Yin, J.-J.; Feix, J. B.; Hyde, J. S. *Biophys. J.* **1990**, *58*, 255−260.
(29) Yin, J.-J.; Subczynski, W. K. *Biophys. J.* **1996**, *71*, 832−839.